Chapter 6

The Bow Shock and the Magnetosheath

The solar wind plasma travels usually at speeds which are faster than any fluid plasma wave relative to the magnetosphere. Therefore a standing shock wave forms around the magnetosphere just as in front of an aircraft traveling at supersonic speeds. The bow shock is the shock in front of the magnetosphere and the magnetosheath is the shocked solar wind plasma. Therefore it is not directly the solar wind plasma which constitutes the boundary of the magnetosphere but the strongly heated and compressed plasma behind the bow shock. The region is rich in various wave phenomena, boundaries and shocks are often treated as discontinuities.

6.1 Solar Wind

Solar coronal outflow: static atmosphere

In a steady state with radial outflow the solar wind must satisfy continuity, momentum, and energy equations

$$\frac{d}{dr}\left(r^2 n v\right) = 0 \tag{6.1}$$

$$v\frac{dv}{dr} = -\frac{GM}{r^2} - \frac{1}{m_i n}\frac{dp}{dr} \tag{6.2}$$

$$\frac{d}{dr}\left(\frac{p}{n^\gamma}\right) = 0 \tag{6.3}$$

with the gravitational constant G and the solar mass M.

Exercise: Derive the above equation from the set of MHD equations

The first solutions of these equations have assumed a static plasma (Chapman) yielding from (6.2) and (6.3)

$$-\frac{GM}{r^2} - \frac{1}{m_i n}\frac{dp}{dr} = 0 \tag{6.4}$$

$$\frac{d}{dr}\left(\frac{p}{n^\gamma}\right) = 0 \tag{6.5}$$

The energy equation can be written as

$$\begin{aligned} \frac{d}{dr}\left(\frac{p}{n^\gamma}\right) &= \frac{1}{n^\gamma}\frac{dp}{dr} - \gamma\frac{p}{n^{\gamma+1}}\frac{dn}{dr} = 0 \\ \frac{d}{dr}\left(\frac{p}{n^\gamma}\right) = \frac{m}{\gamma}\frac{d}{dr}\left(\frac{c_s^2}{n^{\gamma-1}}\right) &= -\frac{\gamma-1}{\gamma}m_i\frac{c_s^2}{n^\gamma}\frac{dn}{dr} + \frac{1}{\gamma}m_i\frac{1}{n^{\gamma-1}}\frac{dc_s^2}{dr} = 0 \end{aligned}$$

with $c_s^2 = \gamma p/m_i n = \gamma k_B T/m_i$ which yields

$$\frac{dp}{dr} = m_i c_s^2 \frac{dn}{dr} \tag{6.6}$$

$$\frac{\gamma-1}{n}\frac{dn}{dr} = \frac{1}{c_s^2}\frac{dc_s^2}{dr} \tag{6.7}$$

or

$$\frac{1}{n}\frac{dp}{dr} = \frac{m_i}{\gamma-1}\frac{dc_s^2}{dr} \tag{6.8}$$

and substitution into the force balance equation yields

$$\frac{1}{\gamma-1}\frac{dc_s^2}{dr} = -\frac{GM}{r^2}$$

where $c_s^2 = \gamma p/m_i n = \gamma k_B T/m_i$ with the solution

$$T - T_0 = -\frac{\gamma-1}{\gamma}\frac{GM}{k}\left(\frac{1}{r_0} - \frac{1}{r}\right) \tag{6.9}$$

This represents the general solution for gravitational bound atmospheres if the radial velocity can be neglected. The temperature decreases at the so-called adiabatic lapse rate with height. The solution for the pressure p and n can be obtained from (6.3) using the ideal gas law $p = nk_BT$ to relate pressure and temperature. In the special case of constant temperature the force balance equation can be directly integrated yielding

$$p = p_0 \exp\left(\frac{GMm}{2kT}\left(\frac{1}{r} - \frac{1}{R_S}\right)\right) \tag{6.10}$$

Parker's steady state solar wind equation

Using the continuity equation

$$\frac{2}{r} + \frac{1}{n}\frac{dn}{dr} + \frac{1}{2v^2}\frac{dv^2}{dr} = 0$$

in the energy equation (6.6)

$$\frac{2}{r}c_s^2 + \frac{c_s^2}{2v^2}\frac{dv^2}{dr} = -\frac{1}{m_i n}\frac{dp}{dr}$$

Substitution in the force balance equation yields

$$\frac{1}{2}\frac{dv^2}{dr} = -\frac{\Phi}{r} + \frac{2}{r}c_s^2 + \frac{c_s^2}{2v^2}\frac{dv^2}{dr}$$

or

$$\frac{r}{2}\left(v^2 - c_s^2\right)\frac{1}{v^2}\frac{dv^2}{dr} = 2c_s^2 - \Phi$$

Normalization to solar radii R_s with $\Phi_0 = GM/R_S$ and $R = r/R_S$ yields

$$\frac{1}{2}R\left(v^2 - c_s^2\right)\frac{1}{v^2}\frac{dv^2}{dr} = 2c_s^2 - \frac{\Phi_0}{R} \tag{6.11}$$

An alternative form in terms of the sonic Mach number can be obtained by substitution of $v^2 = c_s^2 M_s^2$.

$$\left(\frac{\Phi_0}{R} + K\right)R\frac{M_s^2 - 1}{M_s^2}\frac{dM_s^2}{dr} = \left(1 + \frac{\gamma - 1}{2}M_s^2\right)\left[4K + \frac{3\gamma - 5}{\gamma - 1}\frac{\Phi_0}{R}\right] \tag{6.12}$$

where K is an integration constant. There is no known analytical solution to these equations but it is possible to draw several qualitative conclusions:

For $|M_s| = 1$ the lhs of (6.11) vanishes such that the rhs must also be 0. This sonic point is located at a distance

$$R_c = \frac{\Phi_0}{2c_s^2}$$

To have the sonic point above the solar surface implies $R_c > 1$ or

$$c_s^2 < \frac{\Phi_0}{2}$$

Discussion for $\Lambda = 2c_s^2 - \Phi_0/R$

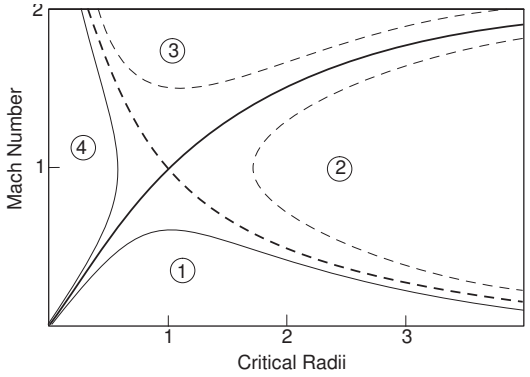

Figure 6.1: The four types of the Parker solution.

(a) $\Lambda < 0$:

i. $v > c_s$ => $dv/dr < 0$

ii. $v < c_s$ => $dv/dr > 0$

and v -> c_s for dv/dr -> $\pm\infty$

(b) $\Lambda > 0$:

i. $v > c_s$ => $dv/dr > 0$

ii. $v < c_s$ => $dv/dr < 0$

c) $\Lambda > 0$: Singularity for $v = c_s$ or $dv/dr = 0$

Properties of the Solar Wind

Typical velocities of the solar wind range between 300 km/s and 1400 km/s with a typical value of about 500 km/s. Source region of the solar wind are the so-called coronal holes, which are region where the magnetic field of the sun stretches out into interplanetary space, i.e., is not closed in a loop back to the sun. In the solar corona the temperature is about $1.6 \cdot 10^6$ K and density about $5 \cdot 10^{17}\ cm^{-3}$.

- Velocities of the solar wind: between 300 km/s and 1400 km/s with a typical value of about 500 km/s.
- Density: decreases from about $10^4 cm^{-3}$ at 0.1 AU to about $5 cm^{-3}$ at 1 AU.
- Temperature: decreases from about 10^6 K at 0.1 AU to about 10^5 K at 1 AU corresponding to approximately 10 eV
- Thermal electron velocity ≈ 1500 km/s and thermal ion velocity 35 km/s
- Magnetic field: about 5 nT
- Alfvén speed: $v_A = B_{sw}/\sqrt{\mu_0 m_i n} \approx 40$ km/s
- Fast mode speed: $c_f = \sqrt{\left(B^2 + \gamma p\right)/\mu_0 m_i n} \approx 60$ km/s
- Plasma $\beta > 1$ often

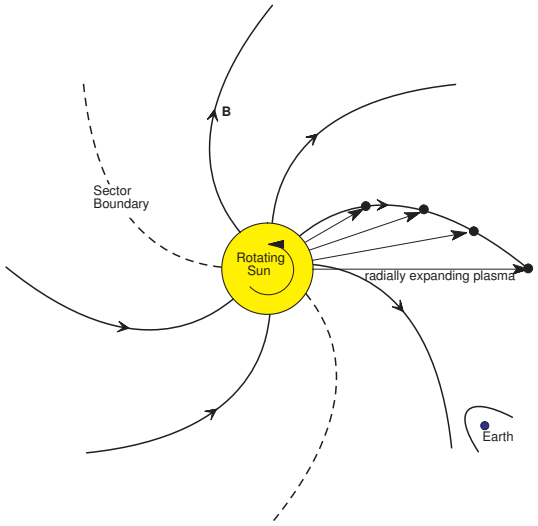

Figure 6.2: Illustration of spiral and sector structure of the solar wind.

Thus the solar wind is much faster than the sound, Alfvén, and fast mode wave speeds in the frame of the Earths. This implies the existence of a shock in front of the magnetosphere - the bow shock - across which the solar wind plasma is decelerated to 'sub-fast' velocities which then interact with the Earth. Caused by the sun's rotation the magnetic field has a spiral shape (Parker spiral configuration) and is usually closely aligned with the ecliptic plane.

6.2 MHD Discontinuities and Shocks

The typical solar wind is much faster than the fastest MHD mode speed $c_f = \sqrt{\left(B^2 + \gamma p\right)/\mu_0 m_i n}$. Similar to supersonic flow past an aircraft the solar wind develops a shock in front of the magnetosphere across which the solar wind is decelerated to velocities below the fast mode speed. In a fluid approximation this shock can be represented as a discontinuity across which mass, momentum, and energy has to be conserved. The jump conditions on large (fluid) scales can be derived from the MHD equations.

6.2.1 Rankine Hugoniot Conditions and MHD Discontinuities

To derive the jump conditions across a fluid boundary it is assumed that this boundary is infinitesimally thin and that the system is in a stationary state. The assumption of zero width is equivalent to assuming a one-dimensional boundary. Assuming a property which is conserved

$$\frac{\partial f}{\partial t} = -\nabla \cdot f\mathbf{u} \tag{6.13}$$

these assumption imply $fu_n = const$ where u_n is the velocity normal to the discontinuity. Another way to express this result is

$$[fu_n] \equiv f_d u_{nd} - f_u u_{nu} = 0 \tag{6.14}$$

where the indexes d and u indicate the downstream and upstream regions. It is easy to show that $[ab] = \frac{1}{2}\langle a\rangle [b] + \frac{1}{2}[a]\langle b\rangle$ where In other words the flux of f is constant across the thin boundary. To apply this method it is convenient to write the basic equation (the set of MHD equations) in a conservative form. This is already the case for the continuity equations. The momentum equation can easily be brought into conservative form and similarly the total energy density (thermal, bulk flow, and magnetic energy) can be expressed in conservative from (implying energy conservation. The complete set of equations which need to be solved are

$$\frac{\partial \rho}{\partial t} = -\nabla \cdot \rho\mathbf{u} \tag{6.15}$$

$$\frac{\partial \rho\mathbf{u}}{\partial t} = -\nabla \cdot \left[\rho\mathbf{u}\mathbf{u} + \left(p + \frac{B^2}{2\mu_0}\right)\underline{\underline{1}} - \frac{1}{\mu_0}\mathbf{B}\mathbf{B}\right] \tag{6.16}$$

$$\frac{\partial w_{tot}}{\partial t} = -\nabla \cdot \left[\left(\frac{1}{2}\rho u^2 + \frac{\gamma p}{\gamma - 1} + \frac{1}{\mu_0}B^2\right)\mathbf{u} - \frac{\mathbf{u}\cdot\mathbf{B}}{\mu_0}\mathbf{B} - \frac{\eta}{\mu_0}\mathbf{j}\times\mathbf{B}\right] \tag{6.17}$$

$$\frac{\partial \mathbf{B}}{\partial t} = \nabla \times (\mathbf{u}\times\mathbf{B} - \eta\mathbf{j}) \tag{6.18}$$

$$0 = \nabla \cdot \mathbf{B} \tag{6.19}$$

with the total energy density

$$w_{tot} = \frac{1}{2}\rho u^2 + \frac{p}{\gamma - 1} + \frac{1}{2\mu_0}B^2 \tag{6.20}$$

Exercise: Derive the conservative form of the momentum equation.

Exercise: Derive the conservative form of the total energy density equation.

Exercise: Why is the electric field energy not considered in the energy equation. $\nabla \cdot \mathbf{B} = 0$ is usually an initial condition. Why is it included in the set of equation to derive the jump conditions.

Using the above set of MHD equations any steady state has to satisfy

$$\nabla \cdot \rho\mathbf{u} = 0 \tag{6.21}$$

$$\nabla \cdot \left[\rho\mathbf{u}\mathbf{u} + \left(p + \frac{B^2}{2\mu_0}\right)\underline{\underline{1}} - \frac{1}{\mu_0}\mathbf{B}\mathbf{B}\right] = 0 \tag{6.22}$$

$$\nabla \cdot \left[\left(\frac{1}{2}\rho u^2 + \frac{\gamma p}{\gamma - 1} + \frac{1}{\mu_0}B^2\right)\mathbf{u} - \frac{\mathbf{u}\cdot\mathbf{B}}{\mu_0}\mathbf{B} - \frac{\eta}{\mu_0}\mathbf{j}\times\mathbf{B}\right] = 0 \tag{6.23}$$

$$\nabla \times (\mathbf{u}\times\mathbf{B} - \eta\mathbf{j}) = 0 \tag{6.24}$$

$$\nabla \cdot \mathbf{B} = 0 \tag{6.25}$$

To obtain the so-called Rankine Hugoniot conditions We now assume a one-dimensional boundary with zero width and assume ideal MHD ($\eta = 0$):

$$\mathbf{n}\cdot[\rho\mathbf{u}] = 0 \tag{6.26}$$

$$\mathbf{n}\cdot[\rho\mathbf{u}\mathbf{u}] + \mathbf{n}\left[p + \frac{\mathbf{B}^2}{2\mu_0}\right] - \frac{1}{\mu_0}\mathbf{n}\cdot[\mathbf{B}\mathbf{B}] = 0 \tag{6.27}$$

$$\mathbf{n}\cdot\left[\left(\frac{1}{2}u^2 + \frac{\gamma p}{(\gamma-1)\rho} + \frac{1}{\mu_0\rho}B^2\right)\rho\mathbf{u}\right] - \frac{1}{\mu_0}\mathbf{n}\cdot[(\mathbf{u}\cdot\mathbf{B})\mathbf{B}] = 0 \tag{6.28}$$

$$\mathbf{n}\times[\mathbf{u}\times\mathbf{B}] = 0 \tag{6.29}$$

$$\mathbf{n}\cdot[\mathbf{B}] = 0 \tag{6.30}$$

Properties:

- Variables: ρ, $\mathbf{u}$, p, $\mathbf{B}$; No variables: 8; No of equations 8
- $[B_n] = 0$ => $B_n = const$
- $[\rho u_n] = 0$ => $\rho u_n = f_n = const$

Classification:

- $[u_n] = 0$ => 'MHD' discontinuity
- $[u_n] \neq 0$ => shock

Applying the 'trivial' properties

$$f_n[u_n] + \left[p + \frac{B_t^2}{2\mu_0}\right] = 0 \tag{6.31}$$

$$f_n[\mathbf{u}_t] - \frac{1}{\mu_0}B_n[\mathbf{B}_t] = 0 \tag{6.32}$$

$$B_n[\mathbf{u}_t] - [u_n\mathbf{B}_t] = 0 \tag{6.33}$$

$$f_n\left[\frac{1}{2}u^2 + \frac{\gamma p}{(\gamma-1)\rho} + \frac{1}{\mu_0\rho}B_t^2\right] - \frac{1}{\mu_0}B_n[\mathbf{u}\cdot\mathbf{B}] = 0 \tag{6.34}$$

Discontinuities: $[u_n] = 0$

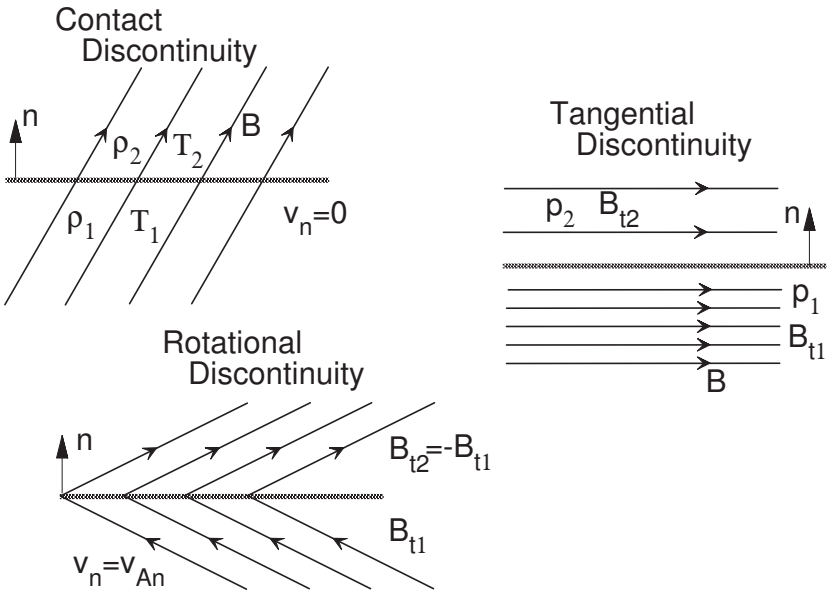

Figure 6.3: MHD discontinuities.

(a) Contact Discontinuity: $u_n = 0$, $B_n \neq 0$ => $[u_t] = 0$, $[B_t] = 0$, $[p] = 0$ => $[\rho] \neq 0$ and $[T] \neq 0$.

(b) Tangential Discontinuity: $u_n = 0$, $B_n = 0$ => $\left[p + \frac{B_t^2}{2\mu_0}\right] = 0$

(c) Rotational Discontinuity: $u_n = const$ => $[\rho] = 0$, $\left[p + \frac{B_t^2}{2\mu_0}\right] = 0$

$$\left.\begin{array}{c} f_n\left[\mathbf{u}_t\right] - \frac{1}{\mu_0} B_n\left[\mathbf{B}_t\right] = 0 \\ B_n\left[\mathbf{u}_t\right] - u_n\left[\mathbf{B}_t\right] = 0 \end{array}\right\} \quad \left(u_n^2 - \frac{B_n^2}{\mu_0 \rho}\right)\left[\mathbf{B}_t\right] = 0$$

=> $u_n^2 = u_{An}^2$ and $\left[\mathbf{u}_t\right] = \pm \frac{u_{An}}{B_n}\left[\mathbf{B}_t\right] = \pm\left[\mathbf{u}_{At}\right]$ with $v_{At} = B_t/\sqrt{\mu_0 \rho}$

tangential direction defined $[B_t]$ with $u_{t1} = u_{At1}$ => $u_{t2} = v_{At2} - v_{At1} + u_{t1} = v_{At2}$

energy equation

$$\left[\frac{\gamma p}{(\gamma - 1)} + \frac{1}{\mu_0} B_t^2\right] = 0$$

=> $[p] = 0$ and $B_{t1} = -B_{t2}$ (or trivial solution $B_{td} = B_{tu}$)

6.2.2 Hydrodynamic Shocks

Formation:

- steepening of large amplitude waves -> compression

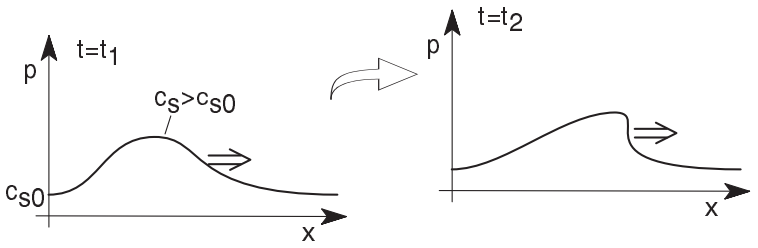

Figure 6.4: Illustration of wave steepening.

- fast motion of an obstacle in a gas or liquid (e.g., aircraft, space shuttle, low altitude satellites)
- waves propagating into a rarefied medium

Equations:

$$n_d u_d = n_u u_u \tag{6.35}$$

$$p_d + m n_d u_d^2 = p_u + m n_u u_u^2 \tag{6.36}$$

$$\left(\frac{1}{2} m n_d u_d^2 + \frac{\gamma}{(\gamma-1)} p_d\right) u_d = \left(\frac{1}{2} m n_u u_u^2 + \frac{\gamma}{(\gamma-1)} p_u\right) u_u \tag{6.37}$$

Introduce: Mach number $M = u/c_s$ with $c_s^2 = \gamma p/mn$

Relations:

$$\frac{n_d}{n_u} = \frac{(\gamma+1)\, M_u^2}{2 + (\gamma-1)\, M_u^2} \tag{6.38}$$

$$\frac{u_d}{u_u} = \frac{n_u}{n_d} \tag{6.39}$$

$$\frac{p_d}{p_u} = \frac{2\gamma M_u^2 - (\gamma-1)}{\gamma+1} \tag{6.40}$$

Entropy (irreversibility):

$$s = c_V \ln \frac{p}{\rho^\gamma} \tag{6.41}$$

with $c_V = \frac{1}{\gamma-1}\frac{k_B}{m} = \frac{3k_B}{2m}$ such that $\Delta s = \Delta s(M_u)$

$$\frac{ds}{dM_u} = \frac{4\gamma\,(\gamma-1)\,(M_u^2-1)\,c_v}{M_u\,[2\gamma M_u^2 - (\gamma-1)]\,[2 + (\gamma-1)\,M_u^2]} \tag{6.42}$$

such that

$$\frac{ds}{dM_u} = 0 \quad for \quad M_u = 1$$

$$\frac{ds}{dM_u} > 0 \quad for \quad M_u > 1$$

Since $s_d = s_u$ for $M_u = 1$ => $s_d > s_u$ for $M_u > 1$ => Entropy must increase for shock!

Shock properties:

- pressure and density increase
- velocity decreases
- entropy increases
- Mach number $M_d < 1$

Strong shocks $M_u \gg 1$ with $\gamma = 5/3$:

$$\frac{n_d}{n_u} = \frac{\gamma+1}{\gamma-1} = 4 \tag{6.43}$$

$$\frac{u_d}{u_u} = \frac{\gamma-1}{\gamma+1} = \frac{1}{4} \tag{6.44}$$

$$\frac{p_d}{p_u} = \frac{2\gamma M_u^2}{\gamma+1} \tag{6.45}$$

$$M_d^2 = \frac{\gamma-1}{2\gamma} = \frac{1}{5} \tag{6.46}$$

6.2.3 MHD Shocks

Coplanarity:

$[u_n] \neq 0$, and $B_n \neq 0$ =>

$$\frac{B_n^2}{\mu_0 f}[\mathbf{B}_t] = [u_n \mathbf{B}_t]$$

Assume $\mathbf{B}_{tu} = B_{tu}\mathbf{e}_y$ such that the z component becomes

$$-\frac{B_n^2}{\mu_0 f} B_{zd} = -u_{nd} B_{zd} \tag{6.47}$$

with the solution $u_{nd} = \frac{B_n^2}{\mu_0 f}$ or $B_{zd} = 0$. Since in general $u_{nd} \neq \frac{B_n^2}{\mu_0 f}$ (except for Alfvén waves) the general solution implies that the tangential fields on the two sides of the shock are aligned

$$\mathbf{B}_{tu} \parallel \mathbf{B}_{td}. \tag{6.48}$$

It follows that $[\mathbf{u}_t] \parallel [\mathbf{B}_t]$. Thus a Galilei transformation can always render the velocities parallel to the magnetic fields.

Basic Equations for MHD Shocks:

Assumptions: $\mathbf{B}_t = B_y \mathbf{e}_y$, $\mathbf{u}_t = u_y \mathbf{e}_y$, and x in the normal $\mathbf{n}$ direction.

$$\rho_d u_{nd} = \rho_u u_{nu} \tag{6.49}$$

$$p_d + \frac{1}{2\mu_0} B_{yd}^2 + \rho_d u_{nd}^2 = p_u + \frac{1}{2\mu_0} B_{yu}^2 + \rho_u u_{nu}^2 \tag{6.50}$$

$$\rho_d u_{nd} u_{yd} - \frac{1}{\mu_0} B_n B_{yd} = \rho_u u_{nu} u_{yu} - \frac{1}{\mu_0} B_n B_{yu} \tag{6.51}$$

$$u_{nd} B_{yd} - u_{yd} B_n = u_{nu} B_{yu} - u_{yu} B_n \tag{6.52}$$

$$\left(\frac{1}{2} \rho_d u_d^2 + \frac{\gamma p_d}{(\gamma - 1)} + \frac{B_d^2}{\mu_0} \right) u_{nd} - \frac{B_n}{\mu_0} \mathbf{u}_d \cdot \mathbf{B}_d = \left(\frac{1}{2} \rho_u u_u^2 + \frac{\gamma p_u}{(\gamma - 1)} + \frac{B_u^2}{\mu_0} \right) u_{nu} - \frac{B_n}{\mu_0} \mathbf{u}_u \cdot \mathbf{B}_u \tag{6.53}$$

Parallel Shock For this case the magnetic field is parallel to the shock normal. The velocity is aligned with the magnetic field and one can always transform into a frame in which $u_y = 0$.

Exercise: Demonstrate that the parallel shock reduces to the pure hydrodynamic shock.

Perpendicular Shock $B_n = 0$. This is a special case we need to discuss because it is not contained in the general solution. Here the magnetic field is exactly perpendicular to the shock.

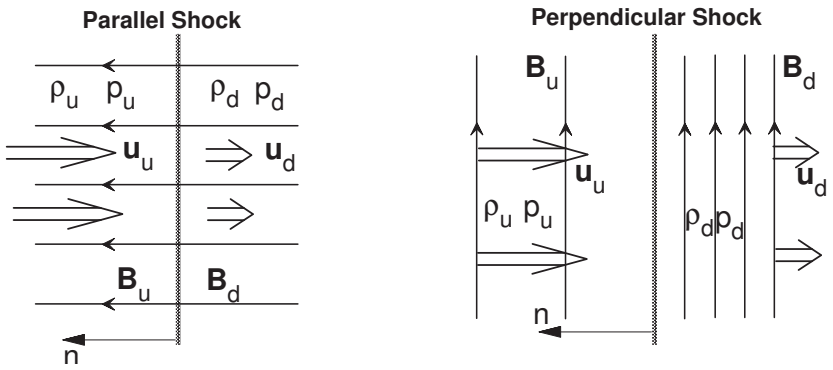

Figure 6.5: Illustration of parallel and perpendicular shocks.

The basic equations reduce to

$$\rho_d u_{nd} = \rho_u u_{nu} \tag{6.54}$$

$$p_d + \frac{1}{2\mu_0} B_{yd}^2 + \rho_d u_{nd}^2 = p_u + \frac{1}{2\mu_0} B_{yu}^2 + \rho_u u_{nu}^2 \tag{6.55}$$

$$\rho_d u_{nd} u_{yd} = \rho_u u_{nu} u_{yu} \tag{6.56}$$

$$u_{nd} B_{yd} = u_{nu} B_{yu} \tag{6.57}$$

$$\left(\frac{1}{2} \rho_d u_d^2 + \frac{\gamma p_d}{(\gamma - 1)} + \frac{B_{yd}^2}{\mu_0} \right) u_{nd} = \left(\frac{1}{2} \rho_u u_u^2 + \frac{\gamma p_u}{(\gamma - 1)} + \frac{B_{yu}^2}{\mu_0} \right) u_{nu} \tag{6.58}$$

Straightforward relations:

$$u_y = 0 \tag{6.59}$$

$$X = \frac{\rho_d}{\rho_u} \tag{6.60}$$

$$\frac{u_{nd}}{u_{nu}} = \frac{1}{X} \tag{6.61}$$

$$\frac{B_{yd}}{B_{yu}} = X \tag{6.62}$$

In addition we use

$$M = \frac{u_u}{c_s} \tag{6.63}$$

$$\beta = \frac{p_{thu}}{p_{Bu}} = \frac{2\mu_0 p_u}{B_u^2} = \frac{2}{\gamma}\frac{c_s^2}{u_A^2} \tag{6.64}$$

$$c_s = \sqrt{\frac{\gamma p}{\rho}} \tag{6.65}$$

$$u_A = \frac{B_u}{\sqrt{\mu_0 \rho_u}} \tag{6.66}$$

From (6.55)

$$\begin{aligned}\frac{p_d}{p_u} &= 1 + \frac{1}{2\mu_0}\frac{B_{yu}^2}{p_u}\left(1 - \frac{B_{yd}^2}{B_{yu}^2}\right) + \frac{\rho_u u_{nu}^2}{p_u}\left(1 - \frac{\rho_d u_{nd}^2}{\rho_u u_{nu}^2}\right) \\ &= 1 + \beta^{-1}\left(1 - X^2\right) + \gamma M^2\left(1 - X^{-1}\right)\end{aligned}$$

and from (6.58)

$$\begin{aligned}\frac{p_d}{p_u} &= \frac{u_{nu}}{u_{nd}} + \frac{\gamma - 1}{2\gamma}\frac{\rho_u u_u^2}{p_u}\left(\frac{u_{nu}}{u_{nd}} - \frac{\rho_d u_{nd}^2}{\rho_u u_{nu}^2}\right) + \frac{\gamma - 1}{\gamma}\frac{B_{yu}^2}{\mu_0 p_u}\left(\frac{u_{nu}}{u_{nd}} - \frac{B_{yd}^2}{B_{yu}^2}\right) \\ &= X + \frac{\gamma - 1}{2}M^2\left(X - X^{-1}\right) + \frac{\gamma - 1}{\gamma}\frac{2}{\beta}\left(X - X^2\right)\end{aligned}$$

Equating the two expressions for p_d/p_u and multiplying with X and dividing by $X - 1$

$$X + \frac{\gamma - 1}{2}M^2\left(X + 1\right) - \frac{\gamma - 1}{\gamma}\frac{2}{\beta}X^2 + \beta^{-1}X\left(1 + X\right) - \gamma M^2 = 0$$

Rearranging this expression X is the positive root of

$$f(X) = 2\left(2 - \gamma\right)X^2 + \left[2\beta + \left(\gamma - 1\right)\beta M^2 + 2\right]\gamma X - \gamma\left(\gamma + 1\right)\beta M^2 = 0 \tag{6.67}$$

Note: Only one positive root!

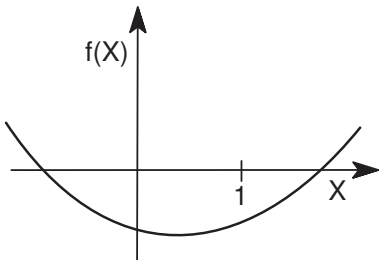

Figure 6.6: $f(X)$ for the shock equation.

(i) Shock must be compressive, i.e., $X \geq 1$ implies $f(1) < 0$.

$$\begin{aligned}f(1) &= 2\left(2 - \gamma\right) + \left[2\beta + \left(\gamma - 1\right)\beta M^2 + 2\right]\gamma - \gamma\left(\gamma + 1\right)\beta M^2 \\ &= M^2\left[\beta\gamma\left(\gamma - 1\right) - \beta\gamma\left(\gamma + 1\right)\right] + 2\left(2 - \gamma + \gamma + \beta\gamma\right) \\ &= -2\beta\gamma M^2 + 2\left(2 + \beta\gamma\right) < 0\end{aligned}$$

=>

$$M^2 \geq 1 + \frac{2}{\gamma\beta} = \frac{c_s^2 + u_A^2}{c_s^2} \tag{6.68}$$

or $u_u^2 \geq c_s^2 + u_A^2$

(ii) Limit $M^2 \gg 1$

$$f(X) = (\gamma - 1)\,\beta M^2 \gamma X - \gamma\,(\gamma + 1)\,\beta M^2 = 0$$

or

$$X = \frac{\gamma + 1}{\gamma - 1} = 4$$

such that

$$\frac{\rho_d}{\rho_u} = 4 \tag{6.69}$$

$$\frac{u_{nd}}{u_{nu}} = \frac{1}{4} \tag{6.70}$$

$$\frac{B_{yd}}{B_{yu}} = 4 \tag{6.71}$$

$$\frac{p_d}{p_u} \approx \frac{5}{4} M^2 \tag{6.72}$$

General Shock Solution

Using a frame of reference with $E_z = -u_x B_y + u_y B_x = 0$ such that

$$u_y = u_n \frac{B_y}{B_n} \tag{6.73}$$

Substitution in (6.49) - (6.53) with $u_{nd} = u_{nu}/X$, $X = \rho_d/\rho_u$, $u_{And}^2 = u_{Anu}^2/X$, and $u_{An} = u_{Anu}$ yields

$$\begin{aligned}
\left(\rho_d u_{nd}^2 - \frac{1}{\mu_0} B_n^2\right) B_{yd} &= \left(\rho_u u_{nu}^2 - \frac{1}{\mu_0} B_n^2\right) B_{yu} \\
&\textit{or} \\
\frac{B_{yd}}{B_{yu}} &= \frac{u_{nu}^2 - u_{An}^2}{u_{nd}^2 - u_{And}^2} \frac{\rho_u}{\rho_d} = \frac{u_{nu}^2 - u_{An}^2}{u_{nu}^2 - X u_{Anu}^2} X \\
\frac{B_{yd}}{B_{yu}} &= \frac{u_u^2 - u_A^2}{u_u^2 - X u_A^2} X
\end{aligned} \tag{6.74}$$

The last result uses the property that the magnetic field and velocity are parallel (i.e., $u_n/u = B_n/B$, and the same for u_{An}). This also implies from Ohm's law $u_y/\left(B_y u_n\right) = 1/B_n = const$

$$\begin{aligned}
\frac{u_{yd}}{u_{yu}} &= \frac{B_{yd}}{B_{yu}} \frac{u_{nd}}{u_{nu}} \\
&= \frac{u_u^2 - u_A^2}{u_u^2 - X u_A^2}
\end{aligned} \tag{6.75}$$

The last two terms in the energy equation

$$\left(\frac{B_{yd}^2+B_n^2}{\mu_0}\right)u_{nd}-\frac{B_n}{\mu_0}\mathbf{u}_d\cdot\mathbf{B}_d=\left(\frac{B_{yd}^2+B_n^2}{\mu_0}\right)u_{nd}-\frac{B_n}{\mu_0}\left(u_{nd}\frac{B_{yd}^2}{B_n}+u_{nd}B_n\right)=0$$

Such that

$$p_d+\frac{1}{2\mu_0}B_{yd}^2+\rho_d u_{nd}^2 = p_u+\frac{1}{2\mu_0}B_{yu}^2+\rho_u u_{nu}^2 \quad (6.76)$$

$$\left(\frac{1}{2}\rho_d u_d^2+\frac{\gamma p_d}{(\gamma-1)}\right)u_{nd} = \left(\frac{1}{2}\rho_u u_u^2+\frac{\gamma p_u}{(\gamma-1)}\right)u_{nu} \quad (6.77)$$

remain to be solved. The energy equation yields

$$\begin{aligned}\frac{p_d}{p_u} &= -\frac{\gamma-1}{2\gamma}\frac{\rho_d u_d^2}{p_u}+\frac{u_{nu}}{u_{nd}}\left(1+\frac{\gamma-1}{2\gamma}\frac{\rho_u u_u^2}{p_u}\right)\\ &= -\frac{\gamma-1}{2}\frac{\rho_d u_d^2}{\rho_u c_{su}^2}+X\left(1+\frac{\gamma-1}{2}\frac{u_u^2}{c_{su}^2}\right)\\ &= X+\frac{\gamma-1}{2}\frac{Xu_u^2}{c_{su}^2}\left(1-\frac{u_d^2}{u_u^2}\right)\end{aligned}$$

Finally

$$p_d+\frac{1}{2\mu_0}B_{yd}^2+\rho_d u_{nd}^2=p_u+\frac{1}{2\mu_0}B_{yu}^2+\rho_u u_{nu}^2$$

$$\begin{aligned}\frac{p_d}{p_u} &= 1+\gamma\frac{u_{nu}^2}{c_{su}^2}\left(1-\frac{\rho_d u_{nd}^2}{\rho_u u_{nu}^2}\right)+\frac{1}{\beta_u}\left(1-\frac{B_{yd}^2}{B_{yu}^2}\right)\\ &= 1+\gamma M_u^2\left(1-X^{-1}\right)+\frac{1}{\beta_u}\left(1-X^2\left(\frac{u_u^2-u_A^2}{u_u^2-Xu_A^2}\right)^2\right)\end{aligned}$$

Combining the pressure equations yields

$$X\left[1+\frac{\gamma-1}{2}\frac{1}{c_{su}^2}\left(u_u^2-u_d^2\right)\right]=1+\gamma M_u^2\left(1-X^{-1}\right)+\frac{1}{\beta_u}\left(1-X^2\left(\frac{u_u^2-u_A^2}{u_u^2-Xu_A^2}\right)^2\right)$$

with u_{yd}^2 from (6.75).

Introducing the angle θ between the incident magnetic field and the shock normal $\mathbf{n}$, X is the solution of

$$\begin{aligned}&\left(u_u^2-Xu_A^2\right)^2\left[Xc_s^2+\frac{1}{2}u_u^2\cos^2\theta\left\{X\left(\gamma-1\right)-\left(\gamma+1\right)\right\}\right]\\ &+\frac{1}{2}u_A^2u_u^2X\sin^2\theta\left[\left(\gamma+X\left(2-\gamma\right)\right)u_u^2-Xu_A^2\left(\left(\gamma+1\right)-X\left(\gamma-1\right)\right)\right] = 0\end{aligned} \quad (6.78)$$

Relations:

$$\frac{\rho_d}{\rho_u} = X \tag{6.79}$$

$$\frac{u_{nd}}{u_{nu}} = \frac{1}{X} \tag{6.80}$$

$$\frac{u_{yd}}{u_{yu}} = \frac{u_u^2 - u_{Au}^2}{u_u^2 - X u_{Au}^2} \tag{6.81}$$

$$\frac{B_{yd}}{B_{yu}} = \frac{u_u^2 - u_{Au}^2}{u_u^2 - X u_{Au}^2} X \tag{6.82}$$

$$\frac{p_d}{p_u} = X + \frac{\gamma - 1}{2} \frac{X u_u^2}{c_{su}^2} \left(1 - \frac{u_d^2}{u_u^2}\right) \tag{6.83}$$

Properties:

- (6.78) has 3 solutions
- Intermediate (Alfvén) wave for $X = 1$ and $u_u^2 = u_{Au}^2$
- $X \approx 1$ slow and intermediate waves => shocks for $X > 1$

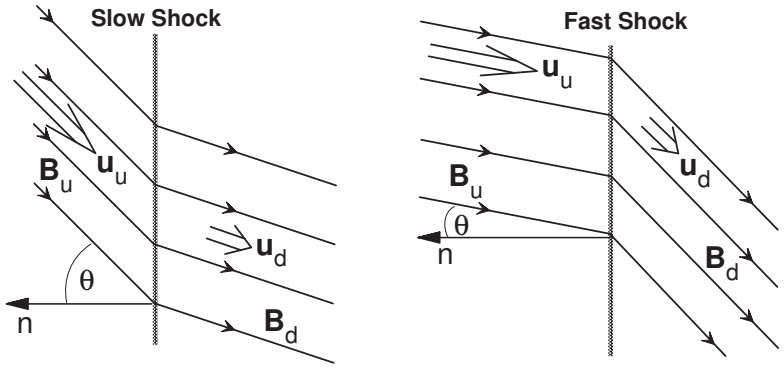

Figure 6.7: Illustration of slow and fast shocks.

Slow and fast shocks:

- Compressive with $X > 1$ => $p_d > p_u$
- Sign of B_y conserved for
  - $u_u^2 \leq u_{Au}^2$ => $B_{yd} < B_{yu}$ and $u_{yd} < u_{yu}$ - slow shock
  - $u_u^2 \geq X u_{Au}^2$ => $B_{yd} > B_{yu}$ and $u_{yd} > u_{yu}$ - fast shock
- limit B_n -> 0
  - fast: B_{yd}/B_{yu} -> X perpendicular shock
  - slow: -> TD

Two special cases of slow and fast shocks are switch-on and switch-off shocks

(a) Switch-off (slow) shock

$$u_u = u_{Au} \tag{6.84}$$

() => $B_{yd} = 0$ tangential magnetic field is switched off!

Since $\mathbf{u}_u \parallel \mathbf{B}_u$ it follows that

$$u_{nu} = \frac{B_{nu}}{\sqrt{\mu_0 \rho_u}} = u_{An} \tag{6.85}$$

=> switch-off shock propagates at Alfvén speed. With the above relations the shock equation becomes

$$\begin{aligned} (1-X)^2 \left[X \frac{c_s^2}{u_A^2} + \frac{1}{2} \cos^2\theta \left\{ X(\gamma-1) - (\gamma+1) \right\} \right] \\ + \frac{1}{2} X \sin^2\theta \left[\gamma + X(2-\gamma) - X(\gamma+1) + X^2(\gamma-1) \right] &= 0 \end{aligned}$$

One can factorize this expression by noting that $X = 1$ is a solution

$$\begin{aligned} (1-X)^2 \left[X \frac{c_s^2}{u_A^2} + \frac{1}{2} \cos^2\theta \left\{ X(\gamma-1) - (\gamma+1) \right\} \right] \\ + \frac{1}{2} X \sin^2\theta \left((X-1)(\gamma X - X - \gamma) \right) &= 0 \end{aligned}$$

or

$$(X-1) \left[2X \frac{c_s^2}{u_A^2} + \cos^2\theta \left\{ X(\gamma-1) - (\gamma+1) \right\} \right] + X \sin^2\theta \left((\gamma-1) X - \gamma \right) = 0$$

Re-arranging yields the equation which has one positive solution

$$\left(2\frac{c_s^2}{u_A^2} + \gamma - 1 \right) X^2 - \left(2\frac{c_s^2}{u_A^2} + \gamma \left(1 + \cos^2\theta \right) \right) X + (\gamma+1)\cos^2\theta = 0 \tag{6.86}$$

Properties:

i. $c_s^2/u_A^2 > 1/2$:

$X \in \left[1,\ 1 + \left(2c_s^2/u_A^2 + \gamma - 1 \right)^{-1} \right]$ (X increases) for $\theta \in [0,\ \pi/2]$

ii. $c_s^2/u_A^2 < 1/2$:

$X \in \left[(\gamma+1) / \left(2c_s^2/u_A^2 + \gamma - 1 \right),\ 1 + \left(2c_s^2/u_A^2 + \gamma - 1 \right)^{-1} \right]$ (X decreases) for $\theta \in [0,\ \pi/2]$

Switch-on (fast) Shock

For propagation along the magnetic field we assume

$$B_{yu} = 0 \tag{6.87}$$

$$\theta = 0 \tag{6.88}$$

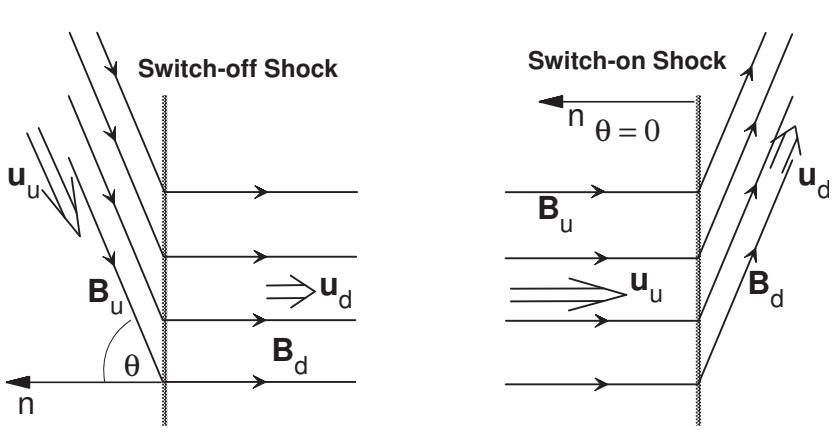

Figure 6.8: Illustration of switch-off and switch-on shocks.

Using this assumption yields the shock equation

$$\left(u_u^2 - X u_A^2\right)^2 \left[X c_s^2 + \frac{1}{2} u_u^2 \left\{X\left(\gamma - 1\right) - \left(\gamma + 1\right)\right\}\right] = 0 \tag{6.89}$$

The slow shock solution is given by $[..] = 0$ and is a purely hydrodynamic shock. The fast shock solution is given by

$$X = \frac{u_u^2}{u_A^2}$$

Eliminating p_d from (6.50) and (6.53) yields B_{yd} as

$$\frac{B_{yd}^2}{B_n^2} = \left(X - 1\right)\left[\left(\gamma + 1\right) - \left(\gamma - 1\right) X - \frac{2\gamma \mu_0 p_u}{B_u^2}\right] \tag{6.90}$$

Since the rhs must be positive the compression ratio must satisfy

$$1 < X < \frac{\gamma + 1 - 2c_s^2/u_A^2}{\gamma - 1} < \frac{\gamma + 1}{\gamma - 1} \tag{6.91}$$

This implies that the field ratio is largest for $c_s^2 \ll u_A^2$ and requires $c_s^2/u_A^2 < \left(\gamma + 1\right)/2$.

Finally the general solution also contains the intermediate wave as a solution with $X = 1$

Summary of shock properties:

- $\rho_d > \rho_u$
- $p_d > p_u$
- $s_d > s_u$
- $\mathrm{sign}\, B_{yd} = \mathrm{sign}\, B_{yu}$

Slow shocks:

- $u_u^2 \leq u_A^2$

- $B_{yd} < B_{yu}$
- $B_d < B_u$
- $u_{yd} < u_{yu}$
- special case: switch-off shock
  - $u_{nu} = \pm u_{An}$
  - $B_{yd} = 0$
  - Strongest compression for $c_s^2/u_A^2 \ll 1$, maximum $X = 4$

Fast Shocks

- $u_u^2 \geq X u_A^2$
- $B_{yd} > B_{yu}$
- $B_d > B_u$
- $u_{yd} > u_{yu}$
- compression increases with Mach number
  - special case: switch-on shock
  - $B_{yd} = 0$
  - Strongest compression for $c_s^2/u_A^2 \ll 1$, maximum $X = 4$

6.3 Properties of the Bow Shock and the Magnetosheath

6.3.1 Foreshocks and deHoffmann-Teller Frame

With the MHD plasma approximation one can analyze basic shock structure and determine downstream conditions as a function of the upstream solar wind properties. We have argued that the reason for the formation of the bow shock is the super fast solar wind speed and that no information can travel upstream from a fast shock. However, considering a kinetic plasma this is not anymore true. In particular any Maxwellian distribution will not only contain thermal particle but also particle although few which have much higher energies than implied by the thermal motion.

To study the dynamics of particles in the vicinity of a fast shock it is instructive to use the deHoffmann-Teller frame, i.e., a frame of reference in which the shock is at rest and the electric field is 0. We have used this frame already in deriving the general shock equation.

Usually it is simple to identify the upstream velocity normal to the shock plane $\mathbf{u}_{nu}$. Moving with this velocity the upstream electric field is 0. However, from our derivation we know that the downstream electric field is nonzero. To transform into the deHoffmann-Teller frame in which the upstream and

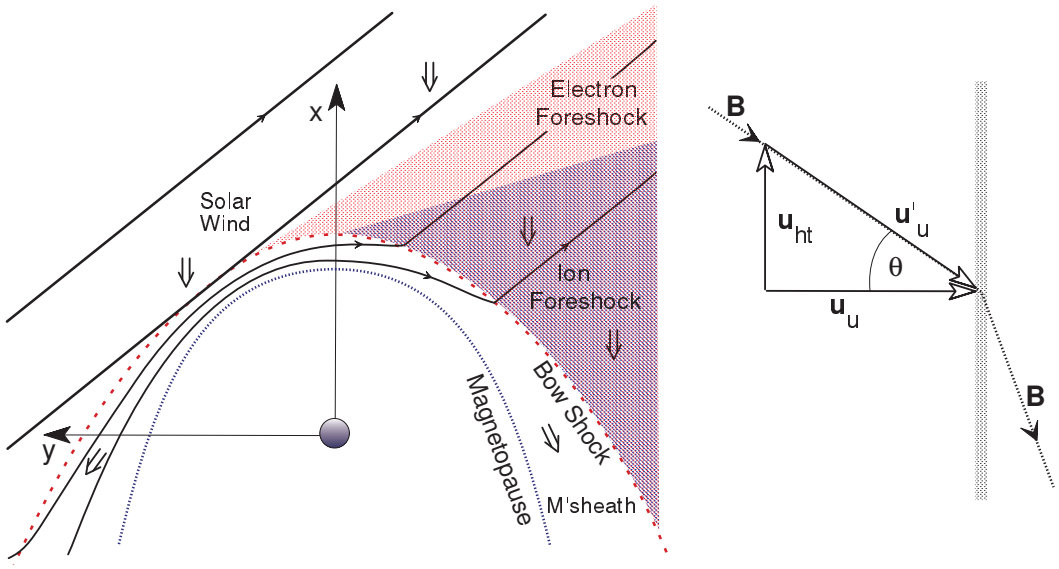

Figure 6.9: Illustration of foreshocks and the deHoffmann-Teller frame.

the downstream electric field is zero and the flow is aligned with the magnetic field on both sides we need a transformation by the deHoffmann-Teller velocity $\mathbf{v}_{ht}$. From Figure (6.9) we see that

$$v_{ht} = u_{nu} \tan\theta \tag{6.92}$$

where θ is the angle between the shock normal and the upstream magnetic field. As θ approaches 90° the deHoffmann-Teller velocity increases rapidly and approaches relativistic values. For $\theta = 90^\circ$ there is no deHoffmann-Teller frame.

A general expression for $\mathbf{v}_{ht}$ is obtained as follows. For the transformation

$$\mathbf{u}'_u = \mathbf{u}_{nu} - \mathbf{v}_{ht}$$

the electric field $\mathbf{E}' = \mathbf{u}'_u \times \mathbf{B} = 0$ such that

$$\mathbf{v}_{ht} \times \mathbf{B}_u = \mathbf{u}_{nu} \times \mathbf{B}_u$$

Taking the cross product with the shock normal unit vector one obtains $\mathbf{n} \times (\mathbf{v}_{ht} \times \mathbf{B}_u) = \mathbf{v}_{ht}\mathbf{n} \cdot \mathbf{B}_u$ or

$$\mathbf{v}_{ht} = \frac{\mathbf{n} \times (\mathbf{u}_{nu} \times \mathbf{B}_u)}{\mathbf{n} \cdot \mathbf{B}_u} \tag{6.93}$$

In the deHoffmann-Teller frame particles have only the gyro motion and the motion parallel to the magnetic field such that particle motion is much easier to study. Particles can outrun the shock if there velocity is sufficiently large. In the deHoffmann-Teller frame the velocity needed for particle to escape from the shock is $\mathbf{u}'_u$. From Figure (6.9) we see that the marginal escape velocity $u_{esc} = u_{nu}/\cos\theta$. Thus particles moving faster than this velocity can outrun the shock and populate the upstream region. The velocity of these particle is a combination of their upstream velocity and the deHoffmann-Teller velocity (or $\mathbf{E} \times \mathbf{B}$ drift in the upstream region). Since particle with higher velocities move ahead of slower escaping particle an observer would expect to see higher energy particles first or further from the shock.

At the Earth the IMF is often in a Parker spiral configuration (Figure 6.2) implying that it has an angle of in the average 45° with the Sun-Earth line. The last field line which touches the bow shock has a shock angle of $\theta = 90°$. Field lines further downstream have decreasing shock angles. Particles originating from the vicinity of the first field line are the most energetic because only those can escape up stream. The upstream region which is filled with the escaping electrons is called the electron foreshock. Ions appear to escape only if $\theta \leq 70°$ such that they fill a region - the ion foreshock - downstream of the electron foreshock region.

The foreshock regions are highly turbulent. The stream of energetic particles against the incoming solar wind is unstable with respect to many instabilities of the two-stream type. Thus the foreshock regions are rich in many different plasma waves excited by the energetic particles.

6.3.2 Shock Structure and Heating

The typical solar wind is a high-Mach number stream with $M_u \approx 8$ such that the bow shock is a fast magnetosonic shock. This also implies that density and magnetic field jump by almost a factor of 4 at the subsolar (the location closest to the sun) location of the bow shock. This distance from Earth of this location is approximated by

$$R_{bs} = \left(1 + 1.1\frac{n_{sw}}{n_{msh}}\right) R_{mp} \tag{6.94}$$

where $R_{mp}is$ the stand-off distance of the magnetopause (the location where the obstacle 'magnetosphere' begins), n_{sw} is the solar wind number density, and n_{msh} is the number density in the subsolar region in the magnetosheath (downstream of the bow shock).

Away from the subsolar point the shock is curved (Figure 6.9). Because of the curvature the solar wind flow is not anymore exactly normal to the shock and the normal component of the solar wind velocity is given by

$$u_{nu} = \mathbf{n}_{bs} \cdot \mathbf{u}_{sw} = u_{sw} \cos\varphi \tag{6.95}$$

where φ is the angle between the shock normal and the Sun-Earth line (GSM x direction). For a subsolar Mach number of 8 the Mach number is reduced to 1 for $\varphi \approx 80°$. Thus the bow shock is finite in size limited to normal directions with $\varphi < 80°$ and the shock structure changes from the subsolar region to the periphery of the bow shock because the Mach number and the magnetic field and orientation relative to the shock changes.

The changing Mach number has additional implications. High-Mach number shocks are called supercritical with $M > M_c$ and have a different structure than sub-critical $M < M_c$ shocks. The critical Mach number is usually defined as the Mach number for which the downstream velocity is equal to the downstream sound speed. This yields a critical Mach number of $M_c \approx 2.7$. For practical purposes observations indicate a critical Mach number < 2 for the bow shock.

The shock structure is also different for quasi-perpendicular (almost perpendicular) and quasi-parallel shocks. Particles cannot travel far into the upstream region for perpendicular shocks because the gyro motion brings them back into the shock. Typically perpendicular shocks show a shock foot where the magnetic field gradually increases in front of the main shock. Behind the main ramp the shock shows an overshoot with field values slightly larger than the asymptotic downstream values.

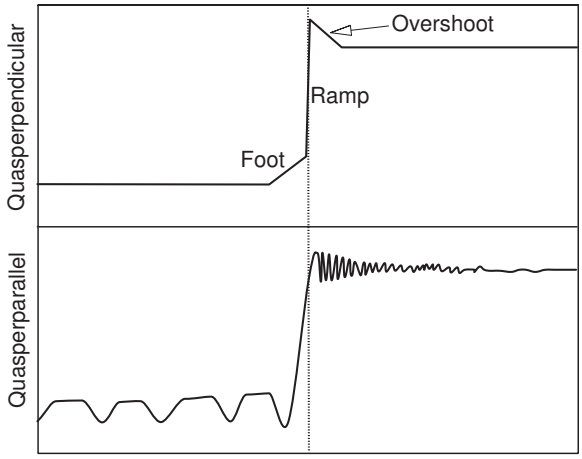

Figure 6.10: Typical magnetic shock profiles.

Quasi-parallel shocks allow a more efficient the escape of particles. Small variations of the upstream magnetic field orientation are amplified by the shock and generate considerable turbulence. In addition - as mentioned - foreshock particles contribute to turbulent fields such that both the upstream and the downstream region show oscillations in the plasma and magnetic field properties.

Shock Currents and Ion Acceleration

A shock leads by definition to an irreversible to heating and compression of the plasma. It therefore requires the presence of irreversible physics such as viscosity or resistivity. The plasma at the bow shock is highly collisionless but the viscous-like or resistive-like processes can occur due the interactions of particles with the turbulent wave fields. However, resistivity and viscosity are insufficient to explain shock structure and typical particle properties such as preferential ion heating. For instance, resistivity would preferentially heat electron. The dissipation in (supercritical) collisionless shock is largely controlled by the actual ion dynamics.

The change in the tangential field $[B_t]$ corresponds to a current in the bow shock

$$j_{sh} = \frac{[B_t]}{\mu_0 l_{sh}} \tag{6.96}$$

where l_{sh} is the width of the shock. This current is equivalent to the increase in the tangential field behind the shock. Because of the larger gyroradii ions can penetrate deep into the compressed field than electrons resulting in a thin layer with an electric field pointing toward the sun. Electrons are accelerated by this electric field into the shock while some ions are can be reflected by this electric field. The electric field is given by

$$\epsilon_0 E_s = e\left(n_{is} + n_{es}\right) l_e$$

where l_eis the width of the electric field layer and n_{is} and n_{es} are ion and electron densities in the layer. Assuming the number of reflected ions as n_{ir} the number of ions in the shock is $n_{is} = n_{es} - n_{ir}$ and the electric field is

$$E_s = \frac{e n_{es} l_e}{\epsilon_0}\left(1 - \frac{n_{ir}}{n_{es}}\right) \tag{6.97}$$

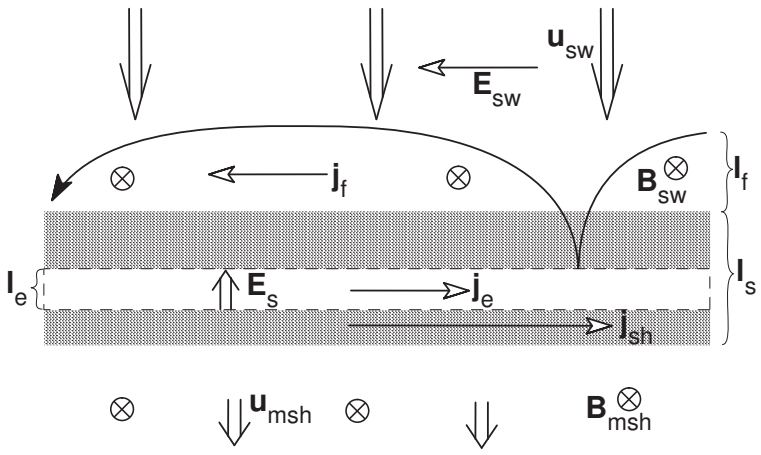

Figure 6.11: Ion motion at a perpendicular shock.

and all ions with energies less than $e\Phi = eE_s l_e$ will be reflected back into the solar wind. In the $\mathbf{E} \times \mathbf{B}$ the reflected ions are accelerated to about twice the solar wind velocity. These reflected ions carry the current observed in the foot region. In addition, the electric field layer causes the electrons to $\mathbf{E} \times \mathbf{B}$ drift while the large gyro-radii for the ions preclude this drift such that the electron carry a (Hall) current in this region.

Note, however, that the interpretation of the current structure based on single particle dynamics and drifts should be considered with care. While the basic shock structure is reasonably represented current based on single particle drifts may not be the correct representation because of diamagnetic (or in general collective) effects which are not included in the single particle dynamics. For instance, the foot current as derived from the particle drift (and acceleration is opposite to the current actually needed for the magnetic field increase at the foot of the shock.

6.3.3 Magnetosheath Flow and Structure

The magnetosheath structure depends strongly on the properties of the bow shock and thus on the upstream solar wind conditions. However, the overall shock location and the flow in the magnetosheath is to lowest order relatively well determined by purely gas dynamic models. But the magnetosheath is a very turbulent medium and there are many source for the turbulent nature of the magnetosheath. The magnetosheath is en entirely open system with a large influx of energy from the solar wind. This is the basic cause for the presence of the turbulence in the magnetosheath. Thus the turbulence is mainly the expression of the many ways that the plasma (at the bow shock and in the magnetosheath) dissipates the energy which is carried into the system by the solar wind. Various aspect of this turbulence are

- kinetic and two-fluid (electrostatic and electromagnetic) plasma waves close to bow shock caused downstream plasma conditions:
  - Whistler
  - Lower-Hybrid
  - Ion-Acoustic
- Non-MHD waves in the magnetosheath.

  - Mirror mode caused by pressure anisotropy.
  - Ion-cyclotron waves driven by electrical current driven.

- Large scale magnetic field fluctuations associated with switch-on (quasi-parallel) shocks.
- MHD wave generation in the bow shock by changes in the upstream solar wind conditions.
- Fast mode wave bouncing between the bow shock and the magnetopause.

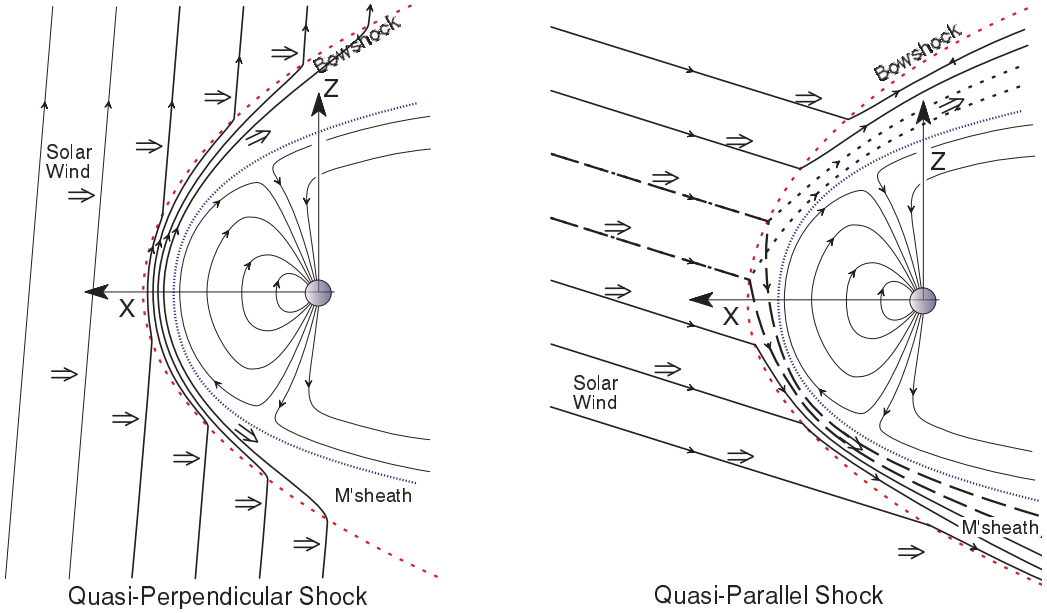

Figure 6.12: Illustration of quasi-perpendicular and quasi-parallel bow shock situations.

Quasi-Perpendicular Shock

A largely perpendicular shock leads to a more pronounced pressure anisotropy with larger perpendicular pressure. The pressure anisotropy can be further enhanced as plasma travels from the bow shock toward the magnetopause because field aligned flow cools the parallel pressure component This has particular importance for the presence of mirror waves in the magnetosheath.

Firehose and Mirror Waves: Low frequency $\omega \ll \omega_{gi}$ and long wavelength $kr_{gi} \ll 1$ limit kinetic waves. Without bulk motion the tensor component $\epsilon_{s2} = 0$ and with $\mathbf{k} = k_{\|}\mathbf{e}_{\|} + k_{\perp}\mathbf{e}_{\perp}$ the dispersion relation splits into

$$\begin{aligned} \frac{k_{\|}^2 c^2}{\omega^2} - \epsilon_{s1} &= 0 \\ \left(\frac{k_{\|}^2 c^2}{\omega^2} + \frac{k_{\perp}^2 c^2}{\omega^2}\right) - \left(\epsilon_{s1} - \epsilon_{s0} + \frac{\epsilon_{s5}^2}{\epsilon_{s3}}\right) &= 0 \end{aligned}$$

The first term reduces to

$$\omega^2 = k_{\|}^2 v_A^2 \left[1 - \frac{1}{2}\sum_s \left(\beta_{s\|} - \beta_{s\perp}\right)\right]$$

This is the kinetic dispersion relation for the so-called fire hose instability. The instability operates when the rhs becomes negative

$$\sum_s \left(\beta_{s\parallel} - \beta_{s\perp}\right) > 2$$

Assuming $\epsilon_{s3} \gg 1$ in the low frequency limit the dispersion relation becomes

$$\left(\frac{k_\parallel^2 c^2}{\omega^2} + \frac{k_\perp^2 c^2}{\omega^2}\right) - (\epsilon_{s1} - \epsilon_{s0}) = 0$$

or with $\zeta_s = \omega/kv_{ths\parallel}$ the dielectric yy component is

$$\epsilon_{yy} = \sum \left\{ \frac{\omega_{ps}^2}{\omega_{gs}^2} - \frac{k_\parallel^2 c^2}{2\omega^2} \left[\beta_{s\perp} - \beta_{s\parallel} + \beta_{s\perp} \frac{k_\perp^2}{k_\parallel^2} \left(2 + \frac{\beta_{s\perp}}{\beta_{s\parallel}} Z'(\zeta_s) \right) \right] \right\}$$

In the very low frequency limit and small phase velocities, $\omega/kv_{thi} \sim \omega/kv_A \ll 1$ one can expand the plasma dispersion function for large arguments which yields

$$i\left(\frac{\pi}{2}\right) \frac{\beta_{i\perp}^2}{\beta_{i\parallel}} \frac{\omega}{kv_{ths\parallel}} = 1 + \sum_s \left(\beta_{s\perp} - \frac{\beta_{s\perp}^2}{\beta_{s\parallel}}\right) + \frac{k_\parallel^2}{k_\perp^2} \left[1 + \frac{1}{2} \sum_s \left(\beta_{s\perp} - \beta_{s\parallel}\right)\right]$$

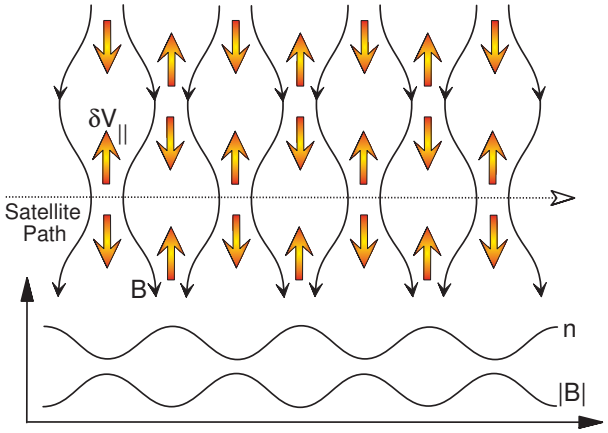

Figure 6.13: Illustration of the mirror mode.

Growth:

Only the ion component contributes to the imaginary part and the frequency is purely imaginary. If the imaginary frequency is negative the mode is purely damped and if it is positive the mode is purely growing. Let us consider two cases:

For strongly **parallel** propagation $k_\parallel^2 \gg k_\perp^2$:

In this case growth occurs if the second term on the rhs becomes negative or

$$\sum_s \beta_{s\parallel} > 2 + \sum_s \beta_{s\perp}$$

which is again the firehose condition.

For strongly **perpendicular** propagation $k_\parallel^2 \ll k_\perp^2$:

Growth occurs for

$$\sum_s \frac{\beta_{s\perp}^2}{\beta_{s\parallel}} > 1 + \sum_s \beta_{s\perp}$$

and the growth rate is

$$\gamma_m = \sqrt{\frac{2}{\pi}} \frac{\beta_{i\parallel}}{\beta_{i\perp}^2} \left[\sum_s \beta_{s\perp} \left(\frac{\beta_{s\perp}}{\beta_{s\parallel}} - 1 \right) - 1 \right] k v_{thi\parallel}$$

- Electrons and ion anisotropy contribute equally to instability
- Growth rate is proportional to ion thermal speed.
- Growth is favored for higher plasma beta $\beta_s = \frac{2\mu_0 p_s}{B_u^2} = \frac{2}{\gamma} \frac{c_s^2}{u_A^2}$

Ion-Cyclotron Waves

Dielectric function for electrostatic plasma waves for propagation with a component parallel to the magnetic field:

$$\epsilon(\omega\, \mathbf{k}) = 1 - \sum_s \sum_{l=-\infty}^{\infty} \frac{\omega_{ps}^2 \Lambda_l(\eta_s)}{k^2 v_{ths}^2} \left[Z'(\zeta_{s.l}) - \frac{2l\omega_{gs}}{k_\parallel v_{ths}} Z(\zeta_{s.l}) \right]$$

with

$$\begin{aligned} \zeta_{i.l} &= \frac{\omega - l\omega_{gi}}{k_\parallel v_{thi}} \\ \zeta_{e.l} &= \frac{\omega - l\omega_{ge} - k_\parallel v_d}{k_\parallel v_{the}} \end{aligned}$$

Here a uniform plasma drift v_d parallel to the magnetic field is assumed for the electron. For purely parallel propagation the dispersion relation also contains ion acoustic wave for $T_e \gg T_i$. For ion cyclotron waves we assume $k_\parallel \ll k_\perp$ and $T_e \approx T_i$ with the solution

$$\omega \approx \omega_{gi} \left[1 + \frac{\Lambda_1(\eta_i)}{1 + T_i/T_e - G} \right]$$

with $G = \Lambda_1 + (1 - \Lambda_0)/\eta_i$, and $\eta_e \ll 1$, $\zeta_{e.l} \ll 1$ and $\zeta_{i.l} \gg 1$ are used. Since $\Lambda_1(\eta_i) < 1$, and $G < 1$ the correction term is usually smaller than 0.5 such that the frequency is close to the ion gyro frequency. In the limit η_i -> 0 the frequency is

$$\omega \approx \omega_{gi} \left(1 + k_\perp^2 c_{ia}^2 / 2\omega 2_{gi} \right) = \omega_{gi} \left(1 + \Delta \right)$$

with $c_{ia}^2 = k_B T_e / m_i$

Onset conditions: Solving for the drift velocity for the unstable wave using the above dispersion relation one can obtain the threshold condition (critical drift velocity) for the growth of ion-cyclotron wave as

$$\frac{v_{dc}}{v_{thi}} = \left(1 + \frac{1}{\Delta(\eta_i^*)} \right) \left\{ \ln \left[2 \left(\frac{m_i T_e}{m_e T_i} \right) \Lambda_1(\eta_i^*) \right] \right\}^{1/2}$$

where η_i^* corresponds to the value of $k_\perp$ where the drift velocity maximizes.

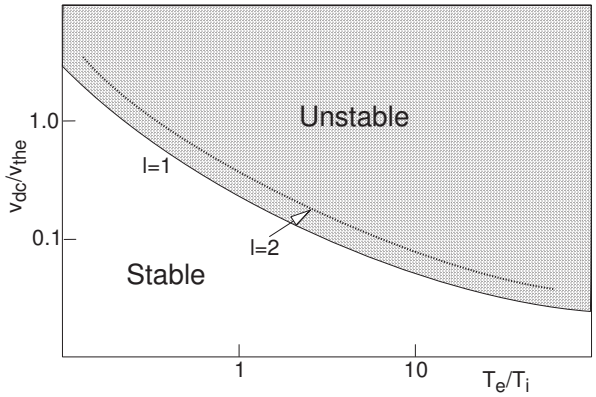

Figure 6.14: Stability of ion-cyclotron waves.

Quasi-parallel shock

We know already that a quasi-parallel shock generates more turbulence both in the upstream and in the down stream region. The shock for $\theta \approx 0$ is a switch-on fast shock. Therefore the downstream magnetic field direction can vary strongly and depends on the history of the plasma and on the small changes in the upstream magnetic field orientation. Thus upstream changes are extremely amplified and small changes can entirely change the magnetosheath magnetic field.

Northward versus southward IMF

Switching the IMF from a northward to a southward direction should not have any influence on the magnetosheath flow and structure if this structure is entirely controlled by the bow shock. Albeit the magnetosheath structure is different for north- and southward fields. A characteristic property of a northward IMF is a region of depleted density and thermal pressure in front of the subsolar magnetopause. This region is absent during periods of strongly southward IMF.

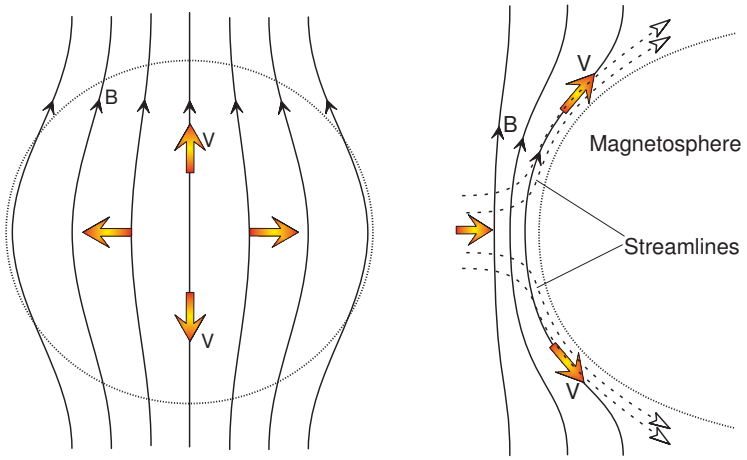

Figure 6.15: Illustration of two- and three-dimensional stagnation flow. The sketch on the left shows a view from the sun onto the dayside magnetopause (circle). The sketch on the right illustrates the flow in a plane determined by the magnetic field orientation and the stagnation flow.

The reason for this difference is magnetic reconnection (which we will discuss later) for the case of southward IMF and a resulting difference in the transport of plasma and vs. the transport of

magnetic flux. The magnetosheath flow and therefore the transport of plasma is three-dimensional, i.e., it occurs in the dawn and dusk directions as well as in the north and south directions as illustrated in Figure 6.15. However, the magnetic flux extends in the north-south direction and for northward IMF it can only be removed by dawn and duskward flow. Thus plasma can be transported more efficiently away from the subsolar region because the removing flow has an additional degree of freedom compared to the flow which can remove the magnetic field.

This may be better illustrated in two dimensions where we assume the Earth to be a cylinder and the magnetosphere a two-dimensional dipole with infinite extend in the GSM y direction. In this situation plasma can still flow around this two-dimensional magnetosphere. However, magnetic flux is stuck in front of the cylinder and cannot be removed if the IMF is northward. Thus the magnetic flux piles up in front of this magnetosphere. For southward IMF reconnection at the dayside magnetopause can disconnect a magnetic field line and remove it from the dayside.

The fact that plasma is more easily removed along the magnetic field for northward IMF leads to an increase in the magnetic flux and magnetic field strength in front of the magnetopause. Pressure balance then requires that the thermal pressure in this region has to decrease giving rise to the so-called plasma depletion layer.

The bow shock as a filter for solar wind perturbations

Thus far we have focused on the stationary structure of the bow shock for given solar wind conditions. However, the solar wind is a relatively unsteady medium. The typical correlation time for solar wind conditions is of the order of 10 to 20 minutes, i.e, solar wind conditions typically change on this time scale. Any perturbation present in the solar wind is transmitted through the bow shock. These perturbations clearly contribute significantly to the turbulent nonlinear waves in the magnetosheath.

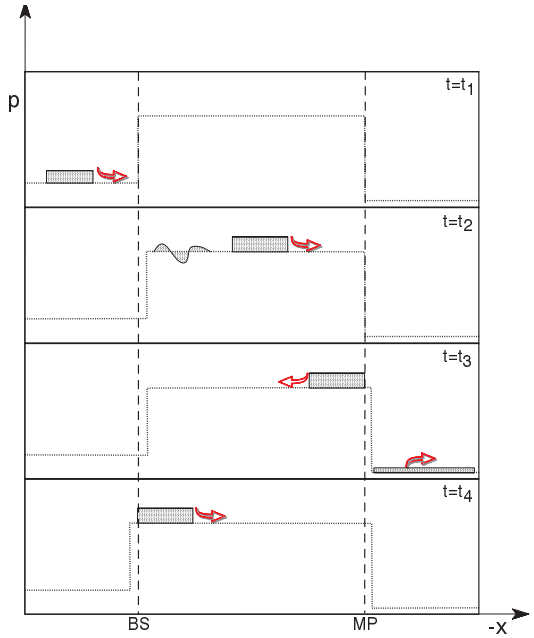

Figure 6.16: Illustration of fast mode bouncing between the bow shock and the magnetopause.

To illustrate the basic aspects of this wave interaction consider a one-dimensional system along the Sun-Earth line. Let us assume that a fast mode rectangular wave pulse travels in the solar wind

toward the Earth. At the bow shock this pulse cannot be reflected such that all energy, momentum, mass, and magnetic flux which is transported by the pulse must be transmitted into the downstream region. During the interaction the plasma condition just upstream of the shock are modified by the wave. Thus shock properties like the compression, tangential field, velocity change. In particular, also the deHoffmann-Teller frame will change implying that the shock location moves up- or downstream depending on the properties of the wave.

The downstream properties are changed because of the intermittent different shock properties. In general the perturbation created downstream cannot be represented by a single rectangular fast wave. Thus the transmitted mass, momentum, energy, and flux transport requires the presence of several MHD waves one o which will be a now modified rectangular fast wave. The fast wave propagates faster downstream than Alfvén and slow waves such that it outruns the other waves. Since the fast mode wave is the only large scale fluid wave with a significant group velocity perpendicular to the magnetic field, the fast wave is the only wave that can reach the magnetopause.

At the magnetopause some of the wave energy is transmitted into the magnetosphere, however most of it is reflected again as fast wave because of the steep density gradient at the magnetopause. During the reflection/transmission other wave modes are generated to maintain mass, momentum, energy, and magnetic flux conservation. The transmitted waves will undergo further modifications and reflections in the magnetosphere. The reflected fast wave is traveling back upstream through the magnetosheath to the bow shock location where it is reflected again with the side effects to move the location of the bow shock again and to generate other MHD wave. In the entire process the amplitude of the fast wave is decreasing because of coupling to other waves, transmission into the magnetosphere, transport in the stagnation flow away from the subsolar region, and because of curvature (three-dimensionality which is not considered in this simplified example.